Journal of Applied Polymer Science

# Nanomechanical properties and thermal stability of recycled cellulose reinforced starch-gelatin polymer composite

**Wendy Rodríguez-Castellanos,[1] Francisco Javier Flores-Ruiz,[1] Fernando Martínez-Bustos,[1] Fernando Chiñas-Castillo,[2] Francisco Javier Espinoza-Beltrán[1]**

[1]Centro de Investigación y de Estudios Avanzados (CINVESTAV) IPN, Unidad Querétaro, Lib. Norponiente 2000, Real de Juriquilla, C.P. 76230, Querétaro Qro, México

[2]Department of Mechanical Engineering, Instituto Tecnológico de Oaxaca, Oaxaca, Oax. Calz. Tecnológico No. 125, CP. 68030, Oaxaca Oax, México

Correspondence to: F. Martínez-Bustos (E-mail: fmartinez@qro.cinvestav.mx)

**ABSTRACT:** Samples of starch−gelatin polymer reinforced with 5% of recycled cellulose were prepared using an extrusion-compression molding process. Nanoindentation and atomic force acoustic microscopy (AFAM) techniques were used to study the effect of reinforcement at nanoscale level. Nanoindentation tests show a 163% increase in hardness and 123% of elastic modulus enhancement after recycled cellulose inclusion. AFAM shows that distribution of recycled cellulose into the polymer matrix is rather homogeneous at nanoscale which improves load transfer. Thermogravimetric analysis indicates an increase in thermal stability of the cellulose reinforced polymer matrix samples. © 2014 Wiley Periodicals, Inc. J. Appl. Polym. Sci. **2015**, *132*, 41787.

**KEYWORDS:** biodegradable; biopolymers and renewable polymers; cellulose and other wood products; extrusion

Received 12 August 2014; accepted 13 November 2014
**DOI: 10.1002/app.41787**

## INTRODUCTION

Production of biodegradable packaging from natural polymers to reduce consumption of synthetic plastics and environmental contamination has been widely investigated.[1–4] Starch-based materials are promising candidates for packaging materials because of its availability, competitive price, and thermoplasticity.[5,6] Mechanical properties of thermoplastic starch (TPS) have been improved adding additives such as plasticizers, cross-linking agents, proteins, antimicrobial agents, antioxidants, and texturizing agents. However, if plasticizer is overused the elastic modulus is reduced due to a phase-separation of the polymer matrix.[7–9] On the other hand, natural fibers have been used as reinforcement, improving the elastic modulus and decreasing hygroscopicity and plasticizing effect of water.[10–13]

In nature, starch, protein, and cellulose are combined to form stable structures as cereal grains. The formation of such structures involves interfacial compatibility between mixtures of hydrophobic and hydrophilic polymers.[14] When a grain is broken, the cracks propagate through the starch granules, not at the interface starch−protein, although when cereal flour is processed by extrusion it is not possible to have a material with the same mechanical properties and complex interfaces as the original grain. Guessama *et al.*[15] have studied the mechanical properties of continuous and dispersed phase in starch–zein composite materials using nanoindentation, reporting a break in the modulus and hardness near the interface. This behavior indicated that there is a lack of adhesion between components, resulting in fragility. Bourmaud *et al.*[16] demonstrated that the mechanical behavior of biocomposites reinforced with vegetable fibers depend of morphology and mechanical properties of fibers.

Nanoindentation has been used to obtain mechanical properties from synthetic fibers such as glass fibers or carbon fibers.[17–20] More recently this technique was used to evaluate elastic modulus and hardness of natural fibers and its anisotropy.[21,22] Similarly, this technique was successfully applied to study the effect of the reinforcement in polymers.[23–25]

Atomic force microscopy (AFM) has been used in the study of polymers to obtain topography images,[25–30] determine average surface roughness,[16,24,31,32] hardness and apparent friction coefficient[33] and estimate the interfacial interaction strength at the interface between a polymer monolayer and a solid substrate.[34] Atomic force acoustic microscope (AFAM) is used to map the elastic modulus distribution of hard surfaces having variations in composition by an ultrasonic frequency that is applied to the tip or sample, providing maps of stiffness which can be converted to elastic modulus map.[35–41]

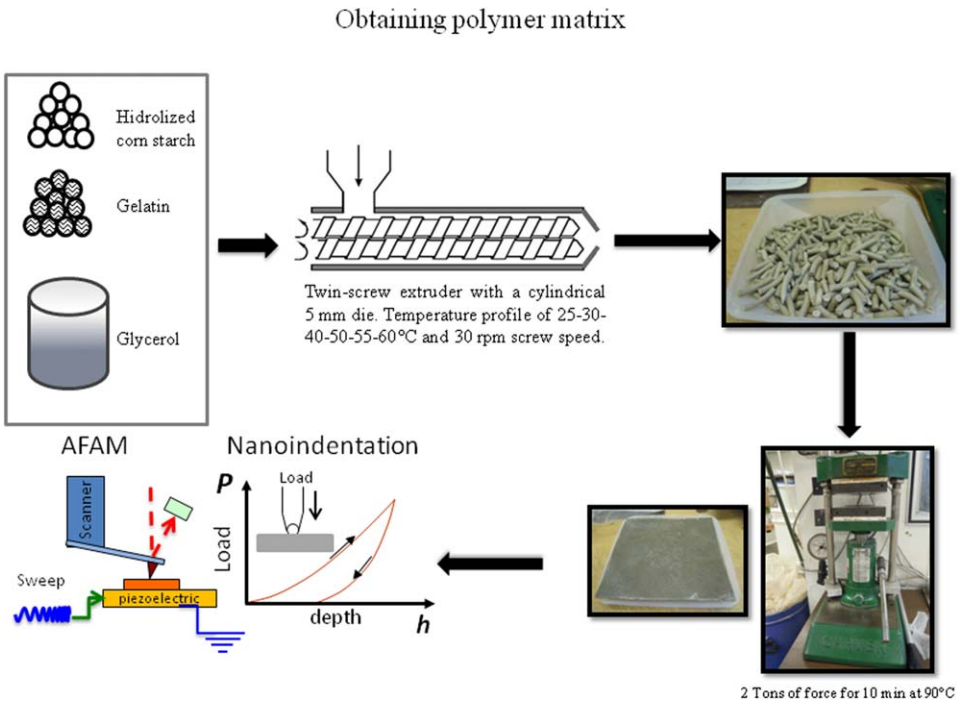


**Figure 1.** Preparation and analysis procedure of starch−gelatin polymer matrix. For more details of the AFAM system see Ref. 45. [Color figure can be viewed in the online issue, which is available at wileyonlinelibrary.com.]

In this work, the mechanical properties of composite samples of recycled cellulose reinforced starch−gelatin polymer (RC-SG) were evaluated at the nanoscale by nanoindentation and atomic force acoustic microscopy (AFAM), in order to study the interaction between starch−gelatin to develop biodegradable packaging materials.

## EXPERIMENTAL

### Polymer Matrix Preparation

Starch−gelatin samples (SG) were used as biopolymer matrix and prepared with hydrolyzed commercial corn starch (ALMEX SA de CV, Guad., Mex.) adding gelatin (Products Cranbury, NJ) and glycerol (Sigma Aldrich St-Louis, MI) (Figure 1). Pellets were produced in a 5 mm diameter air cooled die twin-screw extruder (Thermo Scientific Haake PolyLab OS system, Germany) with a temperature profile of 25–30–40–50–55–60°C and screw speed of 30 rpm as reported in Ref. 42. After that, rectangular samples of 11.5 cm × 11.5 cm × 2 cm were produced using a compression molding technique in a heating press (Carver Mini C press, Wabash, In. USA) of 2 Tons force for 10 min at 90°C.

The same procedure was followed for the starch−gelatin reinforced recycled cellulose (RC-SG) samples adding 5% w/w recycled cellulose (Kimberly Clark, SJR, México) to the polymer matrix.

### Structural and Morphological Characterization

**Scanning Electron Microscopy.** Morphology of RC-SG samples was performed on a scanning electron microscope (Phillips® XL30 ESEM, 47 Eindhoven Holland) using environmental mode.

**Nanoindentation Test.** Nanoindentation tests were performed on an IBIS nanoindentation system (Fisher Crips Laboratories) using a three-sided berkovich tip with 200 nm nominal curvature radius. RC, SG, and RC-SG samples of 80 mm diameter were used. Twenty-five indentations were performed on the surface of each sample with a decreasing load from 400 m*N* to 40 m*N* and separation of 50 μm. Calibration of the indenter was performed on polycarbonate standard ($E = 3$ GPa, $H = 0.19$ GPa) according to the procedure described by Alvarado-Orozco *et al.*[43] Hardness and reduced modulus were determined by Oliver and Pharr method.[44]

**Atomic Force Acoustic Microscopy.** A SPM-AFM system (Bruker/Veeco/Digital Instruments Nanoscope IV Dimension 3100) was used to carry out atomic force acoustic microscopy measurements. Diamond-coated silicon AFM probe (BudgetSensors model ContDLC) with nominal length of 450 μm, first resonance frequency of 13 kHz and spring constant of 0.2 *N*/m was used. For an isotropic material, the indentation modulus $M$ is equal to the plane-strain modulus $M = E/(1\text{-}\nu^2)$ where $E$ is Young's modulus. In resonance tracking atomic force acoustic microscopy, the tip of an AFM cantilever is contacted with the surface of a sample. The tip-sample system is excited by sweep of frequencies around of its resonant frequency, from a piezoelectric device coupled to the lower side of the sample. A photodiode detector follows the cantilever vibration sending a feedback signal to a high-frequency lock-in amplifier (HF2LI, Zurich Instruments). The signal is amplified and filtered using the excitation signal as a reference. RT-AFAM is a technique in which a resonant spectrum is taken and stored for each pixel of an image of 256 × 256 pixels. For each experimental resonant spectrum a simple oscillator harmonic model is fitted, this let us obtain maps of observables such as: amplitude, phase, frequency, and *Q*-value as was previously showed by Enriquez-Flores *et al.*[45] From the frequency map is possible to obtain the

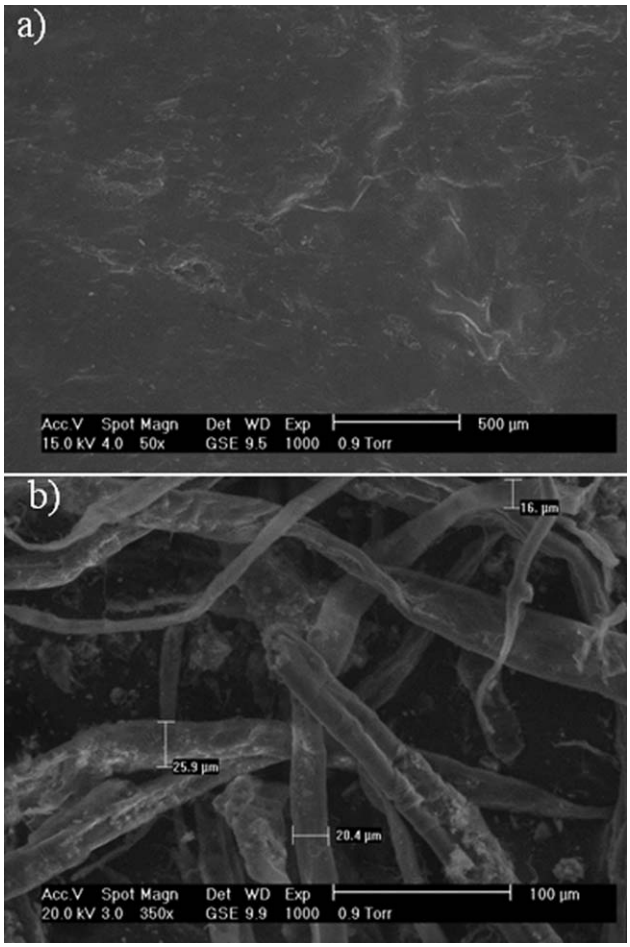


**Figure 2.** SEM micrographs of (a) RC-SG and (b) RC.

resonance frequency shift which are associated to variations in contact stiffness and as a consequence to the indentation modulus of the sample as was showed by Flores-Ruiz *et al.*[39]

### Thermogravimetric Analysis

Thermogravimetric analysis (TGA) allows measure the mass change of a sample as function of temperature in a controlled environment. The loss of weigh of particular sample depends of its stability at temperature change. Thermal stability of samples was measured with a thermogravimetric analyzer Metler Toledo TGA/SDTA 822e (Columbus, OH) taking samples of 5–10 mg using alumina crucibles. All tests were performed in nitrogen environment at a heating rate of 10°C/min between 50°C and 800°C.

## RESULTS AND DISCUSSION

### Scanning Electron Microscopy

A flat disc surface of RC-SG sample prepared by extrusion−compression molding is shown at low magnification in SEM micrograph of Figure 2(a). Details of recycled cellulose presenting diameters of 16–25.9 µm embedded in starch−gelatin matrix were observed in a SEM micrograph at magnification of 350X shown in Figure 2(b).

### Nanoindentation Test Results

Hardness and reduced modulus for this study are showed in Figure 3(a,b), respectively. Nanoindentation measurements indicate that starch−gelatin polymer matrix reinforced with recycled cellulose exhibit higher hardness as shown in Figure 3(a). Cellulose-free SG polymer matrix has a hardness value of 38 MPa whereas adding recycled cellulose rise the hardness up to 100 MPa, thus, approximately an improvement of 163%. Reduced modulus showed an increase of 123% for recycled cellulose reinforced starch−gelatin samples. These results suggest a good adhesion and chemical compatibility between cellulose and starch/gelatin polymer matrix which may have happened during the extrusion process. Cellulose fibers may also be dispersed uniformly during the extrusion, causing an increase in polymer matrix density and, consequently, an improvement in their mechanical properties. In the literature gelatin has been reported to be used as bioadhesive for medical purposes[46,47]; this high adhesion characteristic of cellulose to starch−gelatin polymer matrix may have resulted in higher material hardness. In this respect, hardness values of 86.9 MPa for polyvinyl chloride (PVC) and 118 MPa for polyethylene terephthalate (PET) were reported in Refs. 48 and 49.

In natural polymers, hardness values of 2400 MPa and 640 MPa for gluten and starch respectively, have been reported by Chitchi *et al.*[33] Lee *et al.*[23] registered hardness values of 620 MPa in Lyocell. Additionally, Yun *et al.*[50] measured hardness values of 330 MPa for polyhydroxybutyrate with 1% of carbon nanotubes.

Thermoplastic cornstarch samples processed by injection molding have a hardness value of 141.7 MPa, but after aging for three months this hardness increased to 177 MPa.[51] Hardness of an aged starch is related to starch retrogradation but the starch used in this work was hydrolyzed, thus, retrogradation was lower than native starch. That may explain why hardness values of starch−gelatin polymer matrix were smaller than those reported for thermoplastic corn starch.

Ortiz-Zarama *et al.*[25] recently reported a hardness of 30.7 MPa for gelatin films and 14.0 MPa for carbon nanotubes reinforced gelatin films. This hardness reduction may be because gelatin is a soft polymer as reported by Yun *et al.*[50] Bajardo *et al.*[52] observed an enhancement on nanomechanical properties of the polymer matrix with higher fiber content. These authors conclude that processing parameters affect directly the reduced elastic modulus in polymer materials. In previous work, Zirkel *et al.*[53] reported a reduction in reduced elastic modulus in fluorinated ethylene propylene copolymer foamed films when the processing temperature was increased. The reduced elastic modulus, on the other hand, was higher when pressure was reduced.

### AFAM Quantitative Mapping

Mechanical properties of starch−gelatin plus 5% recycled cellulose (RC-SG) sample at nanoscale were evaluated by AFAM. Topography of the sample under study is shown in Figure 4(a). Map of indentation modulus, exhibited values in the range from 2.1 to 2.7 GPa [Figure 4(b)]. These values are in agreement with those reported by nanoindentation technique. No starch or cellulose fibers are detected as individual material during AFAM test and, as such, surface and indentation modulus both have very slight variations. A reduced elastic modulus indicates that recycled cellulose is dispersing homogeneously

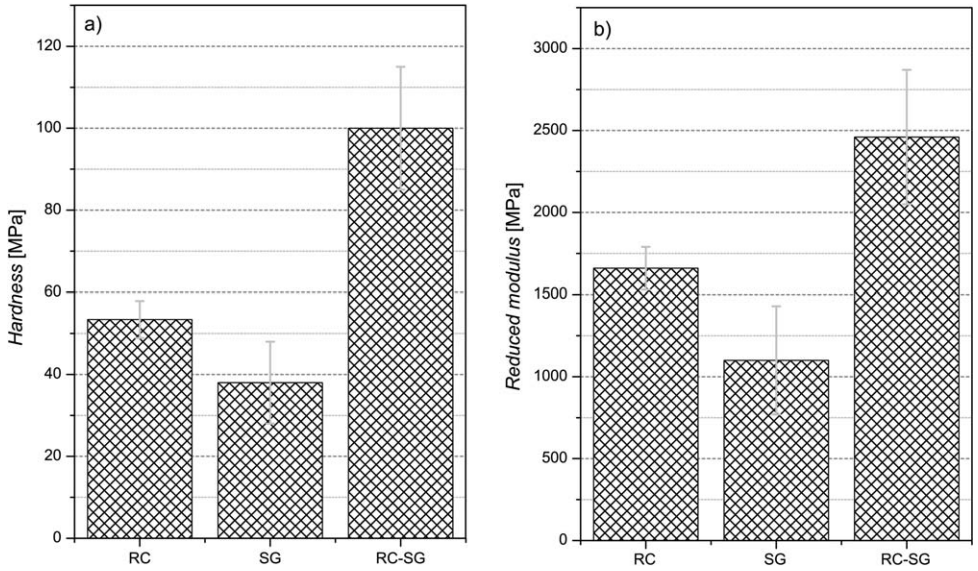


**Figure 3.** (a) Hardness of RC, SG, and RC-SG samples. (b) Reduced elastic modulus of RC, SG, and RC-SG samples.

into starch−gelatin polymer matrix. That behaviour permits a better load transfer, which in turn increases the mechanical and indentation modulus properties of the composite sample. Marinello *et al.*[54] measured Young's modulus of a reinforced polymer composite made of oriented silicon using AFAM technique. These authors reported an error of 5% in thickness measurement between nanoindentation and AFAM. Preghenella *et al.*[55] found that, in epoxy–silica nanocomposites, AFAM results are related to bulk thermo-mechanical data, existing correlation between fracture surfaces and mechanical test.

AFAM histogram in Figure 5 shows that indentation modulus mapping of recycled cellulose reinforced starch−gelatin sample has a maximum value of 2.54 GPa.

### Thermal Stability

Thermal analysis of recycled cellulose in Figure 6 shows an important weight loss between 133 and 330°C, believed to be the result of polymer chains breaking. This thermogram indicates that between 330 and 507°C bonds of glycosides break.

Lerdkanchanaporn *et al.*[56] reported that cellulose degradation starts around 216–542°C and Avicel (a microcrystalline cellulose powder used by both food and pharmaceutical industries) degradation happened between 276.1 and 542.0°C. Hietala *et al.*[57] found recently two degradation steps in kraft pulp fibers, the first in the range of 150–350°C presenting 70% weight loss. The second step is located around the range of 350−525°C, while above 550°C no thermal event occurs. Those previous results are similar to what it was observed in recycled cellulose.

Cellulose free starch−gelatin polymer showed two points of weight loss, the first in the range of 155−267°C and the second in the range of 267−576°C. Kaushik *et al.*[58] indicate that thermal degradation of starch starts at 273°C and cellulose nanofibers starts at 283.2°C. Mu *et al.*[59] report that gelatin films have three points of weight loss, being the first at 23−125°C, related to water present in the film. The second turning point appears at 250°C, being associated with glycerol. Finally, the third inflection point is in the range of 265−460°C linked to gelatin chain degradation. Above 600°C decomposition of thermally stable structures occurred.

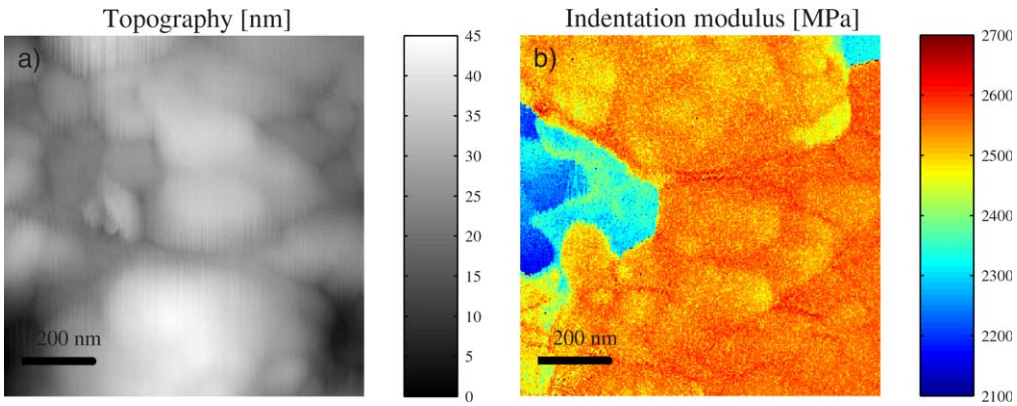


**Figure 4.** (a) Topography image of RC-SG sample. (b) Indentation modulus map of RC-SG sample. [Color figure can be viewed in the online issue, which is available at wileyonlinelibrary.com.]

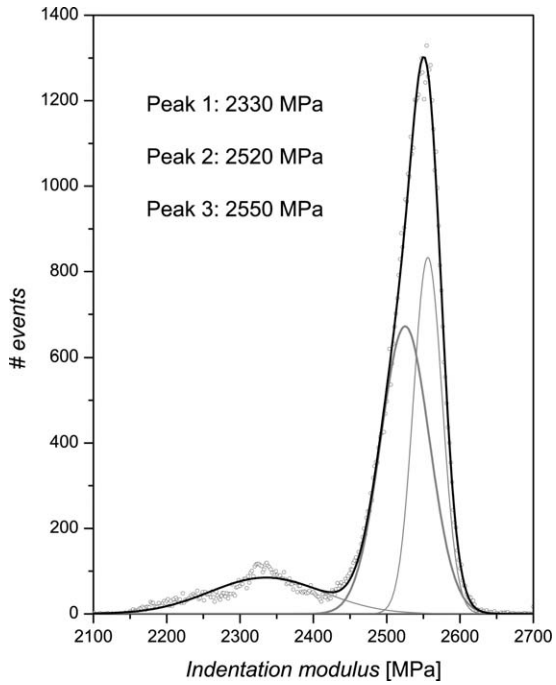


**Figure 5.** Indentation modulus histogram of RC-SG sample.

Thus, in Figure 6, RC-SG thermal analysis shows the first inflection point related to water present in the sample, weight loss is lower than SG sample. Second point is related to thermal degradation of glycerol in the sample. Third inflection point corresponds to total degradation of starch, gelatin and cellulose, being extended slightly above 600°C.

Some authors in previous work state that the addition of micro-nanocellulose improves mechanical, thermal and moisture properties of starch-based materials.[60–62] Xie *et al.* indicate that this effect can not only be attributed to the degree of dispersion or chemical similarity of reinforcement in the polymer matrix, but also to a strong adhesion of hydrogen bonds.[63]

## CONCLUSIONS

Samples of recycled cellulose reinforced starch−gelatin polymer matrix were fabricated using extrusion−compression molding and their mechanical properties and interaction were investigated by nanoindentation, thermogravimetric analysis, and atomic force acoustic microscopy.

Atomic force acoustic microscopy and nanoindentation results showed that polymer matrix reduced elastic modulus and hardness was increased after recycled cellulose addition. The chemical compatibility and adhesion of added cellulose to the polymer matrix forms a nanocomposite that becomes a homogeneous material with better distribution of loads under mechanical test. Thermogravimetric analysis indicated that this material has better thermal stability.

Authors thank Dr. Denis Rodrigue and Yann Giroux from Centre de Recherche sur les Matériaux Avancés (CERMA), Département de Génie Chimique at Laval University in Québec Canada, for their facilities. Authors are also grateful to *Kimberly Clark* de Mexico S.A de C.V. and Dr. Francisco Pérez Robles from Cinvestav-Qro, for providing the recycled cellulose and the National Council for Science and Technology of Mexico (CONACyT) for the scholarship.

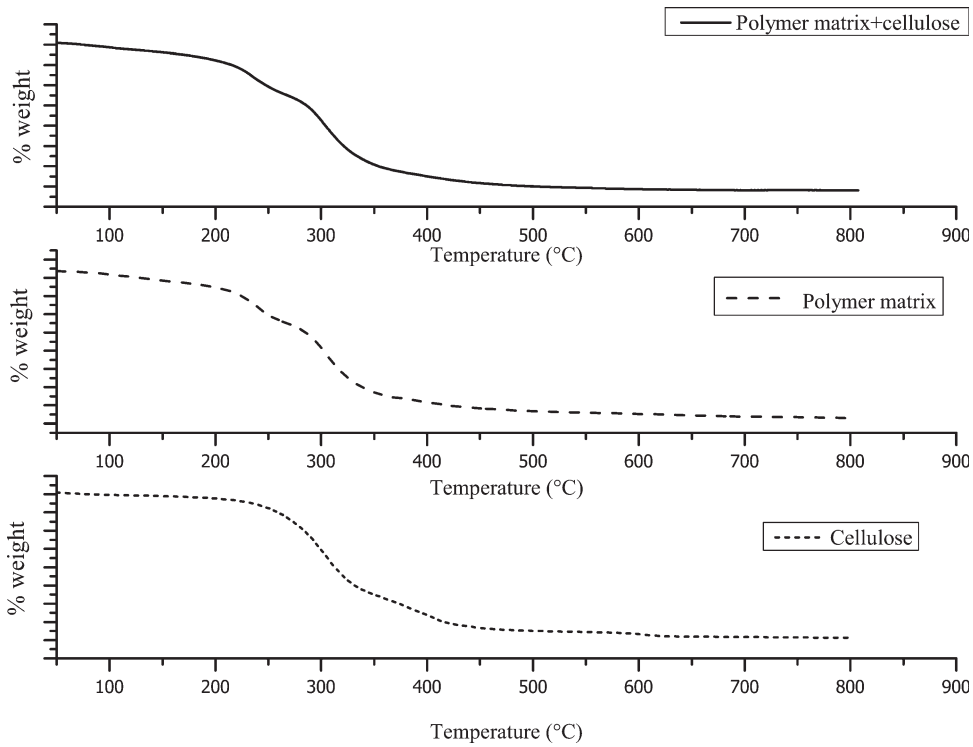


**Figure 6.** TGA Thermogram of samples under study.

## REFERENCES


1. Guilbert, S.; Gontard, N.; Gorris, L. G. M. *LWT Food Sci. Technol.* **1996**, *29*, 10.
2. Pinotti, A.; Garcia, M. A.; Martino, M. N.; Zaritzky, N. E. *Food Hydrocolloids* **2007**, *21*, 66.
3. Hernandez-Izquierdo, V. M.; Krochta, J. M. *J. Food Sci.* **2008**, *73*, R30.
4. Lai, H. M.; Padua, G. W.; Wei, L. S. *Cereal Chem.* **1997**, *74*, 83.
5. Lai, H. M.; Padua, G. W. *Cereal Chem.* **1997**, *74*, 771.
6. Mali, S.; Grossmann, M. V. E.; Garcia, M. A.; Martino, M. N.; Zaritzky, N. Z. *Food Hydrocolloids* **2005**, *19*, 157.
7. Lourdin, D.; Ring, S. G.; Colonna, P. *Carbohydr. Res.* **1998**, *306*, 551.
8. Zhang, Y.; Han, J.; Liu, Z. In Environmental-Compatible Food Packaging; Chiellini, E., Ed.; Woodhead Publishing:, UK, **2008**, p 108.
9. Zhang, Y.; Rempel, C.; Liu, Q. *Crit. Rev. Food Sci. Nutr.* **2014**, *54*, 1353.
10. Lu, Y. S.; Weng, L.; Cao, X. *Macromol. Biosci.* **2005**, *5*, 1101.
11. Ma, X. F.; Yu, J. G.; Wang, N. *Carbohydr. Polym.* **2007**, *67*, 32.
12. Bénézet, J.-C.; Stanojlovic-Davidovic, A.; Bergereta, A.; Ferry, L.; Crespy, A. *Industrial Crops Products* **2012**, *37*, 435.
13. Muller, C. M. O.; Laurindo, J. B.; Yamashita, F. *Food Hydrocolloids* **2009**, *23*, 1328.
14. Leroy, E.; Jacquet, P.; Coativy, G.; Reguerre, A. L.; Lourdin, D. *Carbohydr. Polym.* **2012**, *89*, 955.
15. Guessasma, S.; Sehaki, M.; Lourdin, D.; Bourmaud, A. *Computat. Mater. Sci.* **2008**, *44*, 371.
16. Bourmaud, A.; Baley, C. *Compos. B* **2012**, *43*, 2861.
17. Lonnroth, N.; Muhlstein, C. L.; Pantano, C.; Yue, Y. *J. Non-Crystalline Solids* **2008**, *354*, 3887.
18. do Nascimento, E. M.; Lepienski, C. M. *J. Non-Crystalline Solids* **2006**, *352*, 3556.
19. Gao, S.; Mäder, E.; Zhandarov, S. F. *Carbon* **2004**, *42*, 515.
20. Miyagawa, H.; Mase, T.; Sato, C.; Drown, E.; Drzal, L. T.; Ikegami, K. *Carbon* **2006**, 44, 2002.
21. Wu, Y.; Wang, S.; Zhou, D.; Xing, C.; Zhang, Y.; Cai, Z. *Bioresource Technol.* **2010**, *101*, 2867.
22. Zhang, K.; Si, F. W.; Duan, H. L.; Wang, *J. Acta Biomater.* **2010**, *6*, 2165.
23. Lee, S.-H.; Wang, S.; Pharr, G. M.; Xu, H. *Compos. A* **2007**, *38*, 1517.
24. Kaboorani, A.; Riedl, B.; Blanchet, P.; Fellin, M.; Hosseinaei, O.; Wang, S. *Eur. Polym. J.* **2012**, 48, 1829.
25. Ortiz-Zarama, M. A.; Jiménez-Aparicio, A.; Perea-Flores, M. J.; Solorza-Feria, J. *J. Food Eng.* **2014**, *120*, 223.
26. An, H.; Yang, H.; Liu, Z.; Zhang, Z. *LWT Food Sci. Technol.* **2008**, *41*, 1466.
27. Nair, S. S.; Wang, S.; Hurley, D. C. *Compos. A* **2010**, *41*, 624.
28. Park, H.; Xu, S.; Seetharaman, K. *Carbohydr. Res.* **2011**, *346*, 847.
29. Sujka, M.; Jamroz, *J. LWT-Food Sci. Technol.* **2009**, *42*, 1219.
30. Wang, J.; Somasundaran, P. *J. Colloid Interface Sci.* **2005**, *291*, 75.
31. de Oliveira Romera, C.; de Moraes, J. O.; Zoldan, V. C.; Pasa, A. A.; Laurindo, J. B. *J. Food Eng.* **2012**, *109*, 62.
32. Raj, G.; Balnois, E.; Baley, C.; Grohens, Y. *Colloids Surf. A: Physicochem. Eng. Aspects* **2009**, *352*, 47.
33. Chichti, E.; George, M.; Delenne, J.-Y; Radjai, F.; Lullien-Pellerin, V. *Eur. Polym. J.* **2013**, *49*, 3788.
34. Dvir, H.; Jopp, J.; Gottlieb, M. *J. Colloid Interface Sci.* **2006**, *304*, 58.
35. Rabe, U.; Amelio, S.; Kester, E.; Scherer, V.; Hirsekorn, S.; Arnold, W. *Ultrasonics* **2000**, *38*, 430.
36. Zeng, H. R.; Yu, H. F.; Zhang, L. N.; Chu, R. Q.; Li, G. R.; Yin, Q. R. *Phys. Status Solid. A.* **2005**, *202*, R41.
37. Kumar, A.; Rabe, U.; Hirsekorn, S.; Arnold, W. *Appl. Phys. Lett.* **2008**, *92*, 183106.
38. Zhang, B.; Cheng, Q.; Chen, M.; Yao, W.; Qian, M.; Hu, B. *Ultrasound Med. Biol.* **2012**, *38*, 1383.
39. Flores-Ruiz, F. J.; Reyes-Reyes, J. L.; Chiñas-Castillo, F.; Espinoza-Beltran, F. J. *J. Appl. Polym. Sci.* **2014**, *131*, 40628.
40. Ebert, A.; Tittmann, B. R.; Du, J.; Scheuchenzuber, W. *Ultrasound Med. Biol.* **2006**, *32*, 1687.
41. Passeri, D.; Bettucci, A.; Rossi, M. *Anal Bioanal. Chem.* **2010**, *396*, 2769.
42. Emin, M. A.; Schuchmann, H. P. *J. Food Eng.* **2013**, *115*, 132.
43. Alvarado-Orozco, J. M.; Cardenas-Jaramillo, C.; Torres-Torres, D.; Herrera-Basurto, R.; Hurtado-Macias, A.; Muñoz-Saldana, J.; Trapaga-Martinez, G. *Mater. Res. Soc. Symp. Proc.* **2010**, *18*, 1243.
44. Oliver, W. C.; Pharr, G. M. *J. Mater. Res.* **2004**, *19*, 3.
45. Enríquez-Flores, C. I.; Gervacio-Arciniega, J. J.; Cruz-Valeriano, E.; de Urquijo-Ventura, P.; Gutiérrez-Salazar, B. J.; Espinoza-Beltrán, F. *J. Nanotechnology* **2012**, *23*, 495705.
46. Takaoka, M.; Nakamura, T.; Sugai, H.; Bentley, A. J.; Nakajima, N.; Fullwood, N. J.; Yokoi, N.; Hyon, S.-H.; Kinoshita, S. *Biomaterials* **2008**, *29*, 2923.
47. Wang, T.; Nie, J.; Yang, D. *Carbohydr. Polym.* **2012**, *90*, 1428.
48. Jee, A.-Y.; Lee, M. *Polym. Test.* **2010**, *29*, 95.
49. Curti, P. S.; de Moura, M. R.; Veiga, W.; Radovanovic, E.; Rubira, A. F.; Muniz, E. C. *Appl. Surf. Sci.* **2005**, *245*, 223.
50. Yun, S.; Gadd, G. E.; Latella, B. A.; Lo, V.; Russell, R. A.; Holden, P. *J. Polym. Bull.* **2008**, *61*, 267.
51. Morin-Alcazar, S.; Muñoz-Saldaña, J.; Aguilar-Palazuelos, E.; Jímenez-Arevalo, O.; Ramírez-Bon, R.; Martínez-Bustos, F. *Phys. Status Solid. C* **2007**, *4*, 4242.
52. Baiardo, M.; Zini, E.; Scandola, M. *Compos. A: Appl. Sci. Manufact.* **2004**, *35*, 703.
53. Zirkel, L.; Maier, V.; Durst, K.; Münstedt, H. *Polym. Test.* **2011**, *30*, 286.
54. Marinello, F.; Schiavuta, P.; Vezzùb, S.; Patelli, A.; Carmignato, S.; Savio, E. *Wear* **2011**, *271*, 534.

55. Preghenella, M.; Pegoretti, A.; Migliaresi, C. *Polym. Test.* **2006**, *25*, 443.

56. Lerdkanchanaporn, S.; Dollimore, D.; Alexander, K. S. *Thermochim. Acta* **1998**, *324*, 25.

57. Hietala, M.; Mathew, A. P.; Oksman, K. *Eur. Polym. J.* **2013**, *49*, 950.

58. Kaushik, A.; Singh, M.; Verma, G. *Carbohydr. Polym.* **2010**, *82*, 337.

59. Mu, C.; Guo, J.; Li, X.; Lin, W.; Li, D. *Food Hydrocolloids* **2012**, *27*, 22.

60. Kvien, I.; Sugiyama, J.; Vitrubec, M.; Oksman, K. *J. Mater. Sci.* **2007**, *42*, 8163.

61. Teixeira, E. D. M.; Pasquini, D.; Curvelo, A. A. S.; Corradini, E.; Belgacem, M. N.; Dufresne, A. *Carbohydr. Polym.* **2009**, *78*, 422.

62. Cao, X. D.; Chen, Y.; Chang, P. R.; Stumborg, M.; Huneault, M. A. *J. Appl. Polym. Sci.* **2008**, *109*, 3804.

63. Xie, F.; Pollet, E.; Halley, P. J.; Averous, L. *Prog. Polym. Sci.* **2013**, *38*, 1590.